

# Turbidity as a proxy for total suspended solids (TSS) and particle facilitated pollutant transport in catchments

Hermann Rügner · Marc Schwientek ·  
Barbara Beckingham · Bertram Kuch ·  
Peter Grathwohl

Received: 6 July 2012 / Accepted: 2 February 2013 / Published online: 17 February 2013  
© Springer-Verlag Berlin Heidelberg 2013

**Abstract** Transport of hydrophobic organic pollutants in rivers is mainly coupled to transport of suspended particles. Turbidity measurements are often used to assess the amount of suspended solids in water. In this study, a monitoring campaign is presented where the total concentration of polycyclic aromatic hydrocarbons (PAHs), the amount of total suspended solids (TSS), and turbidity was measured in water samples from five neighboring catchments in southwest Germany. Linear correlations of turbidity and TSS were obtained which were in close agreement to the literature data. From linear regressions of turbidity versus total PAH concentrations in water, mean concentrations of PAH on suspended particles could be calculated and these varied by catchment. These values furthermore comprise a robust measure of the average sediment quality in a given catchment. Since in the catchments investigated in this study, PAH concentrations on suspended particles were stable over a large turbidity range (1–114 Nephelometric Turbidity Units), turbidity could be used as a proxy for total PAHs and likely other highly hydrophobic organic pollutants in river water if the associated correlations are established. Based on that,

online monitoring of turbidity (e.g., by optical backscattering sensors) seems very promising to determine annual pollutant fluxes.

**Keywords** Turbidity · Total suspended solids · Hydrophobic pollutants · Particle-facilitated transport · Catchment hydrology

## Introduction

The amount of total suspended solids (TSS) is an important water quality parameter relevant not only for light penetration and ecological productivity (Parkhill and Gulliver 2002) but also for transport of pollutants such as phosphorus (Grayson et al. 1996; Stubblefield et al. 2007; Spackman Jones et al. 2011; Hornsburch et al. 2010), mercury (Kirchner et al. 2011) and hydrophobic organic compounds (Ko and Baker 2004; Schwientek et al. 2013a). TSS may also be linked to risk assessment approaches and water management concepts (Rossi et al. 2013). TSS increases very rapidly during floods, snow melts or mechanical disturbance of sediments in rivers causing pronounced peak fluxes of particles (Fig. 1), and thus, particle-bound pollutants. If such events are missed or only sparsely resolved in time mean annual fluxes of pollutants are poorly accounted for and underestimated (e.g., Gippel 1995; Hornsburch et al. 2010). However, for high-resolution monitoring of particle-bound pollutants in the field, suitable technologies still have to be developed.

Suspended particles in water cause scattering of light leading to turbidity (cloudiness) of the water, which can be measured by optical backscatter sensors (OBSs, turbidity meters) in the field or by so-called nephelometers commonly used in laboratory water analysis. With recent

---

H. Rügner (✉) · M. Schwientek · P. Grathwohl  
Water and Earth System Science (WESS) Competence Cluster,  
C/O Eberhard Karls University of Tübingen,  
Hölderlinstr. 12, 72074 Tübingen, Germany  
e-mail: h.ruegner@uni-tuebingen.de

B. Beckingham · P. Grathwohl  
Center of Applied Geoscience, Eberhard Karls University  
of Tübingen, Hölderlinstr. 12, 72074 Tübingen, Germany

B. Kuch  
Institute of Sanitary Engineering, Water Quality and Solid Waste  
Management, University of Stuttgart, Bandtäle 2,  
70569 Stuttgart, Germany

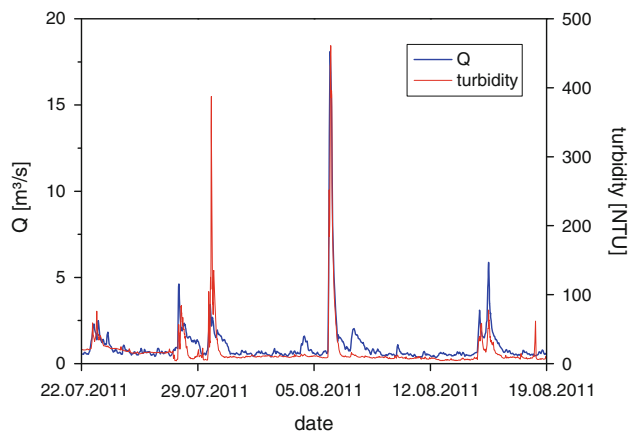


**Fig. 1** Dynamics of discharge ( $Q$ ) and turbidity (reported in nephelometric turbidity units, NTU) measured with an online sensor system (OBS) in one of the catchments investigated in this study (Ammer, at gauge Pfäffingen)

improvements in technology, efforts to equip watersheds with online turbidity sensors are becoming more common. The relationship between turbidity and TSS, however, depends on the size, density, shape and type of the suspended particles in general, as well as on water color (for discussion, see Downing 2006; Gippel 1995; Gray and Glysson 2002). Particle size distribution depends on the flow conditions in rivers, and during strong floods more coarse particles are suspended. The types of particles depend on geology, land use and anthropogenic input (e.g., waste water, surface runoff from agricultural land or urban space). Water color is often affected by dissolved organic carbon (DOC) (e.g., humic acids). Despite all these complications, generally a near-linear relationship is observed for specific field (e.g., Fries et al. 2007) or laboratory datasets. Once calibrated to TSS, the particle flux in rivers could be assessed from turbidity measurements. Moreover, if pollutant concentrations on the suspended particles are

known, or a relationship between particle and pollutant concentrations has been developed, pollutant fluxes can be determined from online turbidity monitoring (see Fig. 1) without the risk to miss events like in routine monthly sampling.

Objectives of this paper are to develop TSS–turbidity relationships from surface water samples taken over a time period of about 1 year in five neighboring catchments in southern Germany. Results are compared with experimental and field data from the literature. To elucidate how this could be used to calculate particle-facilitated pollutant fluxes, particle loads of polycyclic aromatic hydrocarbons (PAHs; used as model compound for the group of hydrophobic organic pollutants) are reported as a function of turbidity. As a next step, the findings of this paper will be used to determine pollutant fluxes using an online sensor network.

## Background

Since particles may control release and transport of a variety of pollutants, turbidity measurements receive much attention, for example, in leaching tests (i.e., of contaminants from soils, recycling/waste and construction materials), in the assessment of the vulnerability of groundwater (e.g., karst systems), and in wastewater treatment. The total concentration  $C_{w,tot}$  of a pollutant in a water sample (e.g., in  $\text{mg l}^{-1}$ ) comprises the “freely” dissolved solute in water ( $C_{w,free}$ ) as well as the amount associated with DOC and the amount bound to suspended particles:

$$C_{w,tot} = C_{w,free} + C_{DOC}f_{DOC} + C_{sus}f_{sus} \quad (1)$$

where  $C_{sus}$  and  $C_{DOC}$  denote the pollutant concentration on suspended particles and associated with DOC (e.g., in  $\text{mg kg}^{-1}$ ), whereas  $f_{sus}$  and  $f_{DOC}$  correspond to the fraction

**Table 1** TSS ( $\text{mg l}^{-1}$ ) versus NTU relationships reported in the literature or calculated from the literature data as shown in Fig. 2

References	$m$ ( $\text{mg l}^{-1} \text{NTU}^{-1}$ )	$R^2$	NTU range	Medium/location
Downing (2006; see Fig. 2)	1.85	0.97	20–320	San Francisco Bay, California
Downing (2006)	1	0.73	10–1,000	Road runoff
Weiß (1998; Fig. 2)	0.48	0.99	100–2,000	Kaolinite (lab)
Weiß (1998; Fig. 2)	0.44	0.99	100–2,000	Silt (lab)
Schwarz et al. (2011; Fig. 2)	1.1	0.99	0.1–100	Karst spring (Blautopf), Germany
Lin et al. (2011)	0.75	0.88	<70	High mountain water reservoirs, Taiwan
Uhrich and Bragg (2000)	2.05 <sup>a</sup>	0.91–0.93 <sup>a</sup>	0.1–1,000	North Santiam River basin, Oregon (online sensors)
Thackston and Palermo (2000; Fig. 2)	2.1	0.99	5–200	Lab column data, sediment
Ziegler et al. (2011)	1.38	0.86	>1000	Mae Sa catchment, Thailand
Stubblefield et al. (2007)	3.3 ( $b = -6.54$ )	0.91	<50	Lake Tahoe, California Blackwood Creek
	2.7 ( $b = -5.41$ )	0.95		Lake Tahoe, California Ward Creek

<sup>a</sup> Non-linear relationships; average  $m$  calculated for NTU values of 1, 10 and 100

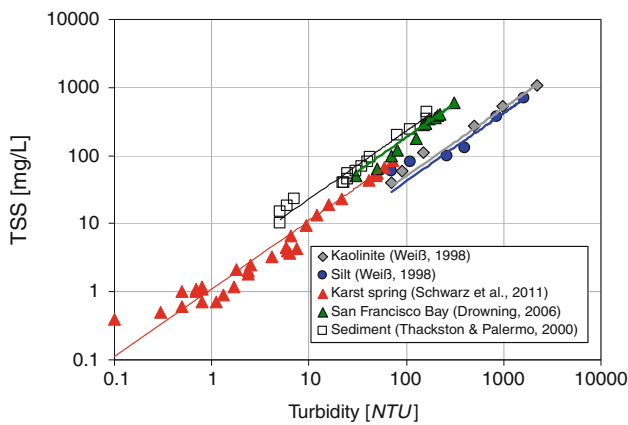


**Fig. 2** Some data and correlations of total amount of suspended solids (TSS) and turbidity measured with light scattering (NTU); for regression data, see Table 1

of suspended particles and organic carbon in water (in  $\text{kg l}^{-1}$ ), respectively.  $C_{\text{DOC}}$  may be expressed as  $C_{\text{w,free}} K_{\text{OC}}$ , where the latter denotes the partition coefficient between water and DOC (e.g., Chiou et al. 1986).

A linear relationship between total water concentration ( $C_{\text{w,tot}}$ ) and  $f_{\text{sus}}$  with the slope  $C_{\text{sus}}$  and the intercept  $C_{\text{w}}$  is obtained, where  $C_{\text{w}}$  includes both the freely dissolved and DOC-associated concentrations ( $C_{\text{w,free}} + C_{\text{DOC}} f_{\text{DOC}}$ ). If  $C_{\text{sus}} f_{\text{sus}} \gg C_{\text{w}}$  then  $C_{\text{w,tot}}$  equals  $C_{\text{sus}} f_{\text{sus}}$  (i.e.,  $C_{\text{sus}} = C_{\text{w,tot}}/f_{\text{sus}}$ ). From  $C_{\text{w}} = C_{\text{w,free}} + C_{\text{w,free}} K_{\text{OC}} f_{\text{DOC}}$  follows  $C_{\text{w}}/C_{\text{w,free}} = 1 + K_{\text{OC}} f_{\text{DOC}}$ . With  $K_{\text{OC}}$  (for fluoranthene, FTN) on the order of  $10^5 \text{ l kg}^{-1}$  and  $f_{\text{DOC}}$  in the sampled streams mostly  $<5 \text{ mg l}^{-1}$  this ratio is  $<1.5$  indicating that DOC-associated pollutants may only contribute significantly to the total concentration in water ( $C_{\text{w,tot}}$ ) at very low turbidities. Note that the ratio  $C_{\text{sus}}$  (slope)/ $C_{\text{w}}$  (intercept) denotes the distribution coefficient  $K_{\text{d}}$ .

The fraction of suspended solids is often represented by turbidity measurements (as a proxy). Optical back-scattering of water samples is measured in the laboratory or by sensor systems in the field. Results are reported as Nephelometric Turbidity Units (NTU) or Formazine Turbidity Units (FNU) depending on the standards used. Several studies report data and relationships between TSS and NTU (Table 1). Figure 2 shows a compilation of the literature data on TSS–turbidity measurements from laboratory investigations (Weiß 1998; Thackston and Palermo 2000) and field data (Schwarz et al. 2011; Downing 2006). Mostly simple linear relationships are reported:

$$\text{TSS} = m \text{ Turbidity (NTU)}. \tag{2}$$

As Table 1 shows, the differences between various linear TSS–NTU relationships from laboratory and field studies are within a factor of 2 and in many cases, 1 NTU corresponds roughly to 1–2  $\text{mg l}^{-1}$  suspended solids. As

the amount of light scattered depends on particle size, shape, color and reflectivity, correlations between TSS and turbidity may depend on location, geology and landscape features. Non-linear power law relationships are reported by Uhrich and Bragg (2000) for three catchments in the Santiam River basin in Oregon with power law exponents of 0.988, 1.04 and 1.08 and an additional bias correction factor. On average their correlations yield increasing values of  $m$  from 1.8, 2.0 and 2.2  $\text{mg l}^{-1} \text{ NTU}^{-1}$  for NTU values of 1, 10 and 100, respectively (e.g., a 10 % increase in  $m$  per order of magnitude in NTU). Sulaiman and Hamid (1993) also published non-linear power law relationships from rivers in Malaysia with high turbidity of larger than 500 NTU and power law exponents  $>1$ . Similarly, Loperfido et al. (2010) report an exponent of 1.25 from a dataset containing maximum turbidity values of 1,000 NTU. Dodds and Whiles (2004) report an exponent of 0.96 for a large dataset with a relatively low mean TSS of 63  $\text{mg l}^{-1}$ . Stubblefield et al. (2007) report TSS–NTU relationships from snowmelts in the Lake Tahoe area with relatively low NTU ( $<50$ ) using negative intercepts of 5 and 6 NTU, respectively (Table 1). It should be noted that for very high loads of suspended sediment ( $>$ several grams per liter), the linear relationships no longer hold. For instance, Grayson et al. (1996) report different correlations for TSS above or below 1  $\text{g l}^{-1}$ , and Gentile et al. (2010) actually report decreasing turbidity during flood events when suspended sediment loads approach 100  $\text{g l}^{-1}$  and above due to a blinding effect on the turbidity meter. Besides significant correlations between NTU and TSS, reasonable correlations between turbidity and bacteria in water are also reported for relatively low NTUs (Huey and Meyer 2010). To summarize, for the conditions commonly observed in natural rivers, a linear (or at least close to linear) relationship of NTU and TSS with slopes of  $\sim 1$ –2.5 may be expected.

## Materials and methods

### Water sampling campaigns

In October 2009 and monthly from June 2010 to May 2011, water samples were taken from up to 34 sampling locations at the Ammer, Goldersbach, Steinlach and Echaz (tributaries of the Neckar River) and the Neckar River itself. For location and characteristics of these catchments, see Grathwohl et al. (2013). Sampling in the Ammer catchment includes locations within subcatchments including the Ammer springs (two furthest upstream sampling locations). In the Steinlach and Goldersbach catchments, samples were collected at several locations along the main river stem whereas single locations were sampled in the Echaz

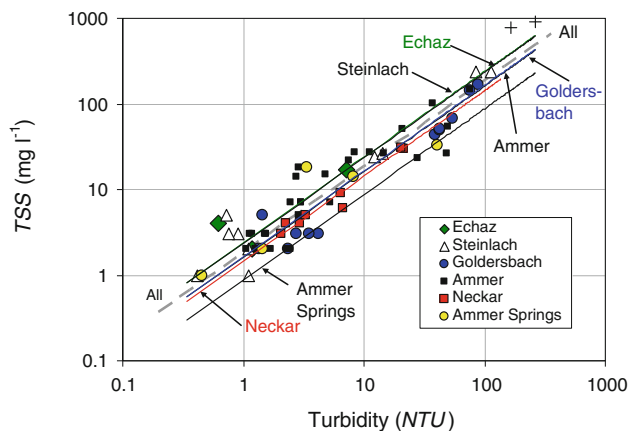


**Fig. 3** Total amount of suspended solids (TSS) versus turbidity of water samples [all catchments:  $\text{TSS} (\text{mg l}^{-1}) = 1.86 (\pm 0.07) \times \text{turbidity} (\text{NTU})$ ; dashed grey line]; TSS values  $>750 \text{ mg l}^{-1}$  from an exceptional flood of the Neckar were not considered in the regression (marked as plus symbol)

(close to the river outlet) and two in the Neckar (just upstream and downstream of the city of Tübingen). In total,  $\sim 350$  samples were taken. Bulk water samples were taken  $\sim 10$  cm below water level, filled into glass bottles (1 or 2 l for PAHs; 1 l for TSS determination; 250 ml for measurements of turbidity and DOC) and stored at  $4^\circ \text{C}$  prior to analysis.

#### Measurement of total suspended solids, turbidity, and DOC

TSS was determined according to the standard guidelines (Standards Methods 2540D 1997) by weighing the dried residues after membrane filtration (glass microfibre,

particle retention  $1.5 \mu\text{m}$ ). TSS was only analyzed in samples taken during the sampling campaigns from October 2010 to January 2011. During October and November 2010, base flow conditions prevailed. December 2010 and January 2011 represent high discharge and declining discharge conditions, respectively, due to the first and second snow-melting events in winter. Turbidity was quantified by a nephelometer (Hach 2100N Turbidimeter) and reported in NTU. Turbidity was monitored for all monthly sampling events from October 2009 and June 2010 to May 2011. Calibration was based on formazine, which is an aqueous suspension of hydrazine sulfate and hexamethylenetetramine. For DOC measurements, filtered samples (particle filter  $0.45 \mu\text{m}$ ) were acidified to pH 2, purged with nitrogen gas and DOC was determined using a TOC analyzer (Elementar High TOC; thermal oxidation at  $680^\circ \text{C}$  and  $\text{CO}_2$  quantification using an IR detector).

#### Analysis of PAHs

Bulk water samples were spiked with a mixture of isotope-labeled standards for quantification purposes ( $10 \mu\text{l}$ , 5 perdeuterated PAHs according to DIN 38407-39 (2008), in toluene, each perdeuterated PAH  $20 \text{ ng } \mu\text{l}^{-1}$ ) and liquid/liquid extracted with cyclohexane. Extracts were then dried with anhydrous sodium sulfate and concentrated to  $100 \mu\text{l}$  for analysis by gas chromatography with mass spectrometer detection (GC/MS) (HP GC 6890 directly coupled with a mass-selective detector Hewlett Packard MSD 5973). Quantification was done by isotope dilution (Boden and Reiner 2004). The detection limit for each compound equaled  $0.001 \mu\text{g l}^{-1}$ . The reported sum of 15 PAHs represents the 16 US EPA priority PAHs excluding naphthalene (NAP).

**Table 2** TSS ( $\text{mg l}^{-1}$ ) versus NTU relationships (this study)

Ref.	$m^a$ ( $\text{mg l}^{-1} \text{NTU}^{-1}$ )	$R^{2b}$	No. <sup>c</sup>	NTU range
All catchments	$1.86 \pm 0.07$	0.89	65	0.4–114
Echaz	$2.39 \pm 0.26$	0.95	3	0.6–7 <sup>d</sup>
Steinlach	$2.35 \pm 0.11$	0.97	10	0.4–114
Goldersbach	$1.65 \pm 0.11$	0.93	12	1–88
Ammer	$1.62 \pm 0.14$	0.75	27	1–76
Neckar	$1.43 \pm 0.05$	0.98	8	2–22 <sup>e</sup>
Ammer Springs	$0.88 \pm 0.20$	0.59	5	0.5–41

<sup>a</sup> Slope ( $\pm$ standard error), intercept was kept at zero

<sup>b</sup> Correlation coefficient

<sup>c</sup> Number of samples

<sup>d</sup> Echaz: a sample  $>50$  NTU was broken and corresponding TSS could not be determined

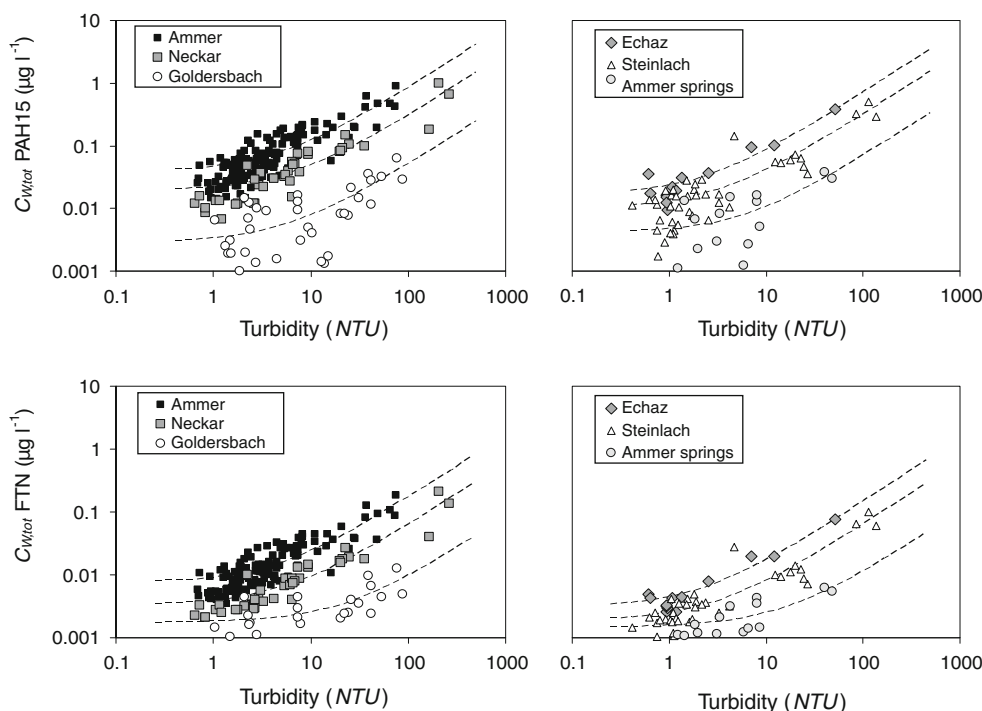
<sup>e</sup> Neckar: two high turbidity samples ( $170 \text{ NTU/TSS} = 780 \text{ mg l}^{-1}$ ;  $260 \text{ NTU/TSS} = 900 \text{ mg l}^{-1}$ ) from an exceptional flood in December 2010 were excluded (linear regression for the Neckar including these values:  $m = 3.75 \pm 0.2 \text{ mg l}^{-1} \text{NTU}^{-1}$ ;  $R^2 = 0.97$ )

## Results

### TSS versus turbidity

Figure 3 indicates good correlations of TSS and turbidity for all catchments. Values for  $m$  are in the range of  $0.9$  (Ammer springs) to  $2.4 \text{ mg l}^{-1} \text{NTU}^{-1}$  (Echaz River; see Table 2). A close correlation was also observed across the five catchments investigated by pooling all data. This result follows probably from the similar geology, climate and landscape of the neighboring catchments. Overall TSS equals 1.86 times the turbidity, which is comparable to the literature values where mostly factors between 1 and 2 have been reported (Table 1). Standard errors of  $m$  are typically below 10%. Thus, turbidity may serve as a proxy for TSS in rivers provided that correlations such as shown in Fig. 3 and Table 2 are determined. However, as for some of the catchments, the number of samples

**Fig. 4** Total concentrations of the sum of 15 PAHs ( $C_{w,tot}$  PAH15) as well as fluoranthene ( $C_{w,tot}$  FTN) versus turbidity from sampling campaigns in October 2009 and June 2010–May 2011. Lines denote linear regressions, intercepts correspond to the total dissolved concentration in water ( $C_w$ ). From slopes and  $m$  values (from TSS–turbidity correlations), average PAH concentrations of suspended particles are obtained (see Table 3)



investigated was limited in the first campaigns, additional measurements might be required to further confirm these correlations. Flow conditions observed during this study ranged from base flow conditions to a high and declining (Neckar, Echaz, and Steinlach) discharge of a flood event with a return period of  $\sim 2\text{--}3$  years. For the specific flood event in the Neckar River in December 2010, TSS values corresponding to turbidity times a factor of 3.5–4.5 were measured (see Fig. 3), indicating that for extreme events, TSS might be underestimated. Investigations concerning the characterization of the suspended materials (e.g., grain size distribution and petrography) might help to explain the observed variability. As even higher turbidity values may be expected [ $>400$  NTU, as shown exemplarily in Fig. 1 for the River Ammer, and which have also been measured in the River Goldersbach and River Steinlach using online turbidity probes (data not shown)], the range observed for

the TSS–turbidity correlation in this study (up to 114 NTU) has to be extended in future work. Although in the Ammer these floods are mainly short-duration events driven by storm water runoff (Schwientek et al. 2013b), they may significantly contribute to annual particle loads. The TSS–turbidity correlations in this study were obtained over fall/winter months from October to January. For this relationship to extend to the full year, particle sources should not have significant seasonal variability.

Total PAH concentrations in water as a function of turbidity

Figure 4 shows relationships between concentrations of 15 PAHs as well as FTN as a representative of the 15 EPA PAHs versus turbidity measured in the water samples for the catchments investigated. Concentrations of 15 PAHs

**Table 3** Slopes and intercepts of linear regressions of  $C_{w,tot}$  versus turbidity) of the data shown in Fig. 4 and average concentrations ( $C_{sus}$ ) of 15 PAHs on suspended sediments ( $\pm$ standard error)

	Echaz	Ammer	Steinlach	Goldersbach	Ammer springs	Neckar
Slope ( $\mu\text{g l}^{-1} \text{NTU}^{-1}$ )	$0.0070 \pm 0.0002$	$0.0080 \pm 0.0004$	$0.0031 \pm 0.0002$	$0.0005 \pm 0.00006$	$0.0007 \pm 0.00011$	$0.0029 \pm 0.0002$
Intercept $C_w$ ( $\mu\text{g l}^{-1}$ )	$0.016 \pm 0.0037$	$0.039 \pm 0.0057$	$0.010 \pm 0.0063$	$0.0029 \pm 0.0016$	$0.0040 \pm 0.0018$	$0.019 \pm 0.015$
$C_{sus}$ ( $\text{mg kg}^{-1}$ )	$2.9 \pm 0.1$	$5.0 \pm 0.2$	$1.3 \pm 0.1$	$0.30 \pm 0.04$	$0.75 \pm 0.1$	$2.0 \pm 0.2$
Log $C_{sus}/C_w$ ( $\text{l kg}^{-1}$ )	5.3	5.1	5.1	4.4	4.9	5.1
$f_{\text{DOC}}$ (mean) ( $\text{mg l}^{-1}$ )	2.5	2.9	3.0	9.4	2.0	4.8
Number of samples	13	139	44	36	15	39

In addition discharge-weighted mean values of dissolved organic carbon ( $f_{\text{DOC}}$ ) are listed

calculated from linear regressions as well as distribution coefficients ( $K_d = C_{sus}/C_w$ ) for fluoranthene;  $C_{sus}$  values were calculated from slopes and the turbidity–TSS correlations ( $m$  values) given in Table 2



and FTN per turbidity unit are the highest in the Ammer, followed by the Echaz, Neckar, Steinlach, Ammer springs and Goldersbach indicating a decreasing pollution of suspended solids in the order specified (Table 3). Notable are the low standard errors which are typically below 10 %. Thus, very robust averages of particle-associated PAH concentrations ( $C_{\text{sus}}$ ) are obtained from the slopes of the linear regressions and the  $m$  values determined from TSS–turbidity correlations. Linear regression more heavily weighs the high turbidities that dominate the pollutant fluxes. Low concentrations observed at low turbidities with relatively large data scatter likely do not contribute significantly to mean annual fluxes of particle-bound pollutants. The concentration of 15 PAHs on suspended particles corresponds with mean concentrations of 15 PAHs measured in the sediments of the River Ammer ( $8.6 \pm 6.5 \text{ mg kg}^{-1}$ , 35 samples). For a further comparison of PAH concentrations on suspended particles with sediments in the Ammer, we refer to Schwientek et al. (2013a).

The intercepts in Fig. 4 correspond to total dissolved concentrations in the surface waters ( $C_w$ ). These relatively low aqueous concentrations as well as the relatively high  $K_d$  values ( $\log C_{\text{sus}}/C_w$ ) for FTN may be explained by non-linearity of sorption at very low aqueous concentrations. For instance, Kleinedam et al. (1999) determined non-linear isotherms (Freundlich model) for phenanthrene in aquifer materials (sandy gravels) from the River Neckar with Freundlich exponents ( $1/n$ ) as low as 0.64 and 0.69 (for grain size fractions  $<0.5 \text{ mm}$ ) leading to  $\sim 10$  times larger distribution coefficients if the concentration decreases by 3 orders of magnitude. Slow desorption kinetics could also contribute to low aqueous concentrations. However, Rügner et al. (1999) showed that, for example, for rock fragments with grain sizes comparable to suspended solids ( $<0.25 \text{ mm}$

in diameter), sorption/desorption equilibrium for phenanthrene is reached within days.

Total PAH concentrations were clearly dominated by  $\geq 3$ -ring compounds. The proportion of NAP in 16 EPA PAHs makes up less than 20 % for  $C_{\text{tot}} > 0.064 \mu\text{g l}^{-1}$  (or  $< 50 \%$  for  $C_{\text{tot}} > 0.031 \mu\text{g l}^{-1}$ ). Although the NAP contribution may be expected to be higher at low water concentrations (due to the higher concentrations of gaseous NAP in the atmosphere compared to other PAHs and the increased fraction of freely dissolved PAH at low turbidities), major uncertainties in the distribution pattern at very low concentrations ( $C_{\text{tot}}$ ) arise from a high NAP concentration in background air in addition to single 3- to 6-ring PAHs being present at concentrations below the detection limits. Calculated  $C_{\text{sus}}$  for 16 EPA PAHs were higher than that for 15 PAH by only 3–5 % in the Ammer, Neckar, Echaz, and Steinlach, but 19 and 47 % in the Ammer springs and Goldersbach, respectively, where  $C_{\text{tot}}$  is the lowest. In addition, PAH patterns were—beyond a very few outliers and the already mentioned analytical uncertainties at very low concentrations—relatively stable over the observed turbidity range and across all catchments investigated (see Fig. 5). This shows that PAHs in surface waters are mainly particle associated and likely originate from old (aged) inputs or diffuse sources.

If at high flow events the composition of particles changes, e.g., by the addition of clean background particles to contaminated urban particles, the relationship between turbidity and pollutant concentration on suspended particles would change as well due to dilution (Schwientek et al. 2013a). However, as it can be also seen in Fig. 4, no systematic deviation of the data from the regression line is observed despite a substantial data scattering at low concentrations. This indicates that the PAH concentrations on

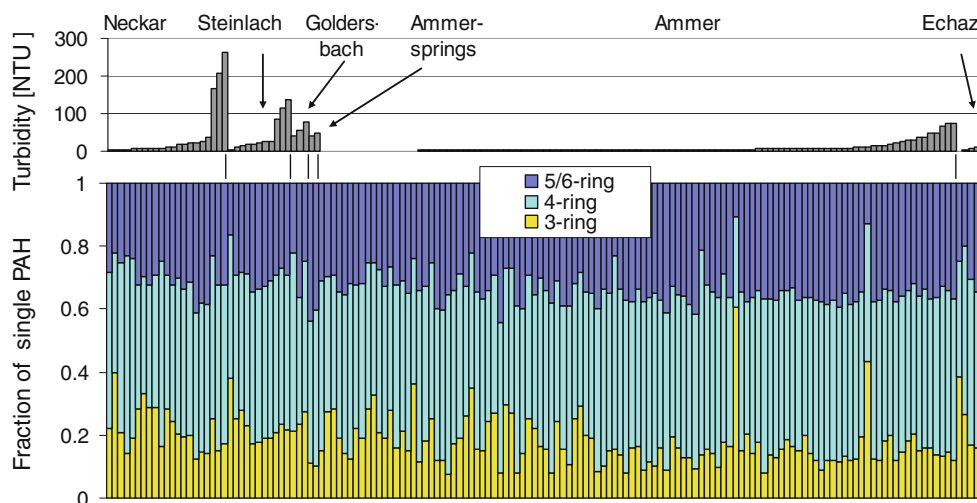


**Fig. 5** Turbidity and distribution patterns of PAHs (3–6-ring). Only samples with concentrations of 15 PAHs ( $C_{w,\text{tot PAH 15}} > 0.03 \mu\text{g l}^{-1}$ ) are displayed (153 out of 286 samples)

suspended solids are approximately constant over the observed turbidity range in the catchments investigated.

It is hypothesized that mainly previously deposited sediments are remobilized by small-to-medium floods and homogenized by the turbulent flow. Thus, contaminant loads of suspended solids could provide an integral signal of sediment pollution in the catchment's stream network. For the samples from the flood event in the River Neckar, TSS was (slightly) underestimated from turbidity (see Fig. 3) and this is likely due to coarser grained particles being mobilized at higher flows. These coarser particles, in many cases, have lower sorption capacity. Illustrating this, Klei-neidam et al. (1999) report Freundlich distribution coefficients for phenanthrene decreasing from 655 to 57 l kg<sup>-1</sup> (determined at 1 µg l<sup>-1</sup>) for increasing grain size fractions (<0.063 to 0.5 mm) in aquifer materials from the River Neckar. This could be mainly attributed to the decrease in organic carbon content in coarser particles. Hence, the underestimation of particle transport at high turbidity may be compensated by a decrease in contaminant loading, and the result is that even the exceptionally high turbidities in River Neckar samples (outliers in Fig. 3) fit quite well to the linear correlation in the C<sub>w,tot</sub> versus turbidity plots (Fig. 4). Therefore, for high turbidity or high flow events, turbidity might be a better proxy than TSS alone. The extent to which the particle composition stays constant in the catchments studied, such as when turbidity increases dramatically with discharge, still has to be clarified. The contribution of different sediment sources during changing flow conditions could vary depending on the catchment and the contaminants of concern. For instance, a decreasing suspended solids concentration of heavy metals with increasing TSS has been observed during high flow storm events (Bradley and Lewin 1982). Furthermore, sampling depth may have an influence on the TSS–turbidity correlation. For instance, Fries et al. (2007) found, in the Neuse River Estuary, a robust correlation for low-salinity surface-water samples, but a poor correlation for samples taken about 0.5 m above the sediment bed, since particles in bottom waters may be primarily derived by resuspension and settling processes which can lead to agglomerated, larger particles which scatter light inconsistently.

### Conclusions

In summary, the results strongly support our proposal to use turbidity as an easy-to-monitor proxy for transport of suspended particles and associated fluxes of hydrophobic pollutants over a broad range of hydrological conditions. The linear correlations hold over a wide range of turbidity and particle-associated pollutant concentration. Notable are the low standard errors typically below 10 % despite

significant data scatter at low pollutant concentrations and turbidities. In principle, laboratory analysis of turbidity and PAH concentrations of only a few bulk water samples allows for a robust measure of the degree of sediment pollution in catchments given that suspended solids may be mainly composed of remobilized sediments during low-to-medium flood events and, therefore, integrate over the heterogeneous sediment pollution patterns. This is a major advantage as assessing sediment pollution in rivers by the conventional sediment sampling and analysis is usually complicated by often very heterogeneous pollutant distributions. The correlations would also allow a relatively precise determination of the mean annual particle-associated pollutant fluxes, since these are dominated by high flow events. Yet the extent to which these proxies may be applied for extreme events or for catchments with different geology is subject to further investigation.

**Acknowledgments** This work was supported by a grant from the Ministry of Science, Research and Arts of Baden-Württemberg (AZ Zu 33-721.3-2) and the Helmholtz Centre for Environmental Research, UFZ, Leipzig.

### References

- Boden AR, Reiner EJ (2004) Development of an isotope-dilution gas chromatographic mass spectrometric method for the analysis of polycyclic aromatic compounds in environmental matrices. *Polycycl Aromat Comp* 24:309–323
- Bradley SB, Lewin J (1982) Transport of heavy metals on suspended sediments under high flow conditions in a mineralized region of Wales. *Environ Pollut (Series B)* 4:257–267
- Chiou CT, Malcolm RL, Brinton TI, Kile DE (1986) Water solubility enhancement of some organic pollutants and pesticides by dissolved humic and fulvic acids. *Env Sci Technol* 20:502–508
- DIN 38407-39 (2008) German standard methods for the examination of water, waste water and sludge; jointly determinable substances (group F)—determination of selected polycyclic aromatic hydrocarbons (PAH)—method using gas chromatography with mass spectrometric detection (GC-MS). August 2008
- Dodds WK, Whiles MR (2004) Quality and quantity of suspended particles in rivers: continent-scale patterns in the United States. *Environ Manag* 33(3):355–367. doi:10.1007/s00267-003-0089-z
- Downing J (2006) Twenty-five years with OBS sensors: the good, the bad, and the ugly. *Cont Shelf Res* 26:2299–2318
- Fries JS, Noble RT, Paerl HW, Characklis GW (2007) Particle suspensions and their regions of effect in the Neuse river estuary: implications for water quality monitoring. *Estuar Coasts* 30: 359–364
- Gentile F, Bisantino T, Corbino R, Milillo F, Romano G, Trisorio Liuzzi G (2010) Monitoring and analysis of suspended sediment transport dynamics in the Carapelle torrent (southern Italy). *Catena* 80:1–8
- Gippel CJ (1995) Potential of turbidity monitoring for measuring the transport of suspended solids in streams. *Hydrol Process* 9:83–97
- Grathwohl P, Rügner H, Wöhling T, Osenbrück K, Schwientek M, Gayler S, Wollschläger U, Selle B, Pause M, Delfs J-O, Grzeschik M, Weller U, Ivanov M, Cirpka OA, Maier U, Kuch B, Nowak W, Wulfmeyer V, Warrach-Sagi K, Streck T, Attinger S, Bilke L, Dietrich P, Fleckenstein JH, Kalbacher T, Kolditz O,

- Rink K, Samaniego L, Vogel H-J, Werban U, Teutsch G (2013) Catchments as reactors—a comprehensive approach for water fluxes and solute turn-over. *Environ Earth Sci* 69(2) doi: [10.1007/s12665-013-2281-7](https://doi.org/10.1007/s12665-013-2281-7)
- Gray JR, Glysson GD (eds) (2002) In: Proceedings of the federal interagency workshop on turbidity and other sediment surrogates. US Geological Survey Circular 1250, Reno, Nevada, 30 April–2 May 2002. [http://pubs.usgs.gov/circ/2003/circ1250/pdf/circ1250.book\\_web.pdf](http://pubs.usgs.gov/circ/2003/circ1250/pdf/circ1250.book_web.pdf)
- Grayson RB, Finlayson BL, Gippel CJ, Hart BT (1996) The potential of field turbidity measurements for the computation of total phosphorus and suspended solids loads. *J Environ Manag* 47:257–267
- Hornsburgh JS, Jones AS, Stevens DK, Tarboton DG, Mesner NO (2010) A sensor network for high frequency estimation of water quality constituent fluxes using surrogates. *Environ Monit Softw* 25:1031–1044
- Huey GM, Meyer ML (2010) Turbidity as an indicator of water quality in diverse watersheds of the upper Pecos river basin. *Water* 2(2):273–284. doi: [10.3390/w2020273](https://doi.org/10.3390/w2020273)
- Kirchner JW, Austin CM, Myers A, Whyte DC (2011) Quantifying remediation effectiveness under variable external forcing using contaminant rating curves. *Environ Sci Technol* 45:7874–7881
- Kleineidam S, Rügner H, Grathwohl P (1999) Slow sorption in heterogeneous aquifer material. *Environ Toxicol Chem* 18: 1673–1678
- Ko FC, Baker JE (2004) Seasonal and annual loads of hydrophobic organic contaminants from the Susquehanna river basin to the Chesapeake bay. *Marine Pollut Bull* 48:840–851
- Lin GW, Chen H, Petley DN, Horng M-J, Wu S-J, Chuang B (2011) Impact of rainstorm-triggered landslides on high turbidity in a mountain reservoir. *Eng Geol* 117:97–103
- Loperfido JV, Just CL, Papanicolaou AN, Schnoor JL (2010) In situ sensing to understand diel turbidity cycles, suspended solids, and nutrient transport in Clear Creek, Iowa. *Water Res* 46:W06525. doi: [10.1029/2009WR008293](https://doi.org/10.1029/2009WR008293)
- Parkhill KL, Gulliver JS (2002) Effect of inorganic sediment on whole-stream productivity. *Hydrobiologia* 472:5–17
- Rossi L, Chèvre N, Fankhauser R, Margot J, Curdy R, Babut M, Barry DA (2013) Sediment contamination assessment in urban areas based on total suspended solids. *Water Res* 47:339–350
- Rügner H, Kleineidam S, Grathwohl P (1999) Long term sorption kinetics of phenanthrene in aquifer materials. *Environ Sci Technol* 33:1645–1651
- Schwarz K, Gocht T, Grathwohl P (2011) Transport of polycyclic aromatic hydrocarbons in highly vulnerable karst systems. *Environ Pollut* 159:133–139
- Schwientek M, Rügner H, Beckingham B, Kuch B, Grathwohl P (2013a) Integrated monitoring of transport of persistent organic pollutants in contrasting catchments. *Environ Pollut* 172: 155–162
- Schwientek M, Osenbrück K, Fleischer M (2013b) Investigating hydrological drivers of nitrate export dynamics in two agricultural catchments in Germany using high-frequency data series. *Environ Earth Sci* 69(2). doi: [10.1007/s12665-013-2322-2](https://doi.org/10.1007/s12665-013-2322-2)
- Spackman Jones A, Stevens DK, Horsburgh JS, Mesner NO (2011) Surrogate measures for providing high frequency estimates of total suspended solids and total phosphorus concentrations. *J Am Water Resour Assoc (JAWRA)* 47(2):239–253
- Standards Methods Organisation (1997) Standards Methods 2540D. <http://www.standardmethods.org/AboutSM/>
- Stubblefield AP, Reuter JE, Dahlgren RA, Goldman CR (2007) Use of turbidimetry to characterize suspended sediment and phosphorus fluxes in the Lake Tahoe basin, California, USA. *Hydrol Process* 21:281–291
- Sulaiman WNA, Hamid MR (1993) Suspended sediment and turbidity relationships for individual and multiple catchments. Universiti Putra, Malaysia, p 132
- Thackston EL, Palermo MR (2000) Improved methods for correlating turbidity and suspended solids for monitoring. In: DOER technical notes collection (ERDC TN-DOER-E8). US Army Engineer Research and Development Center, Vicksburg. <http://el.ercd.usace.army.mil/elpubs/pdf/doere8.pdf>
- Uhrich MA, Bragg HM (2000) Monitoring instream turbidity to estimate continuous suspended-sediment loads and yields and clay-water volumes in the upper north Santiam river basin, Oregon, 1998–2000. USGS water-resources investigations report 03-4098, USA. <http://pubs.usgs.gov/wri/WRI03-4098/>
- Weiß H (1998) Säulenversuche zur Gefahrenbeurteilung für das Grundwasser an PAK-kontaminierten Standorten. *Tübinger Geowissenschaftliche Arbeiten (TGA) Reihe C* 45, p 111
- Ziegler AD, Xi LX, Tantasarin C (2011) Sediment load monitoring in the Mae Sa catchment in northern Thailand. In: Walling DE (ed) *Sediment problems and sediment management in Asian river basins*, 349th edn. IAHS, Wallingford, pp 86–91